CERN-SPSC-2020-012 / SPSC-P-366
08/04/2020

Usage of the CERN MORPURGO magnet for the MADMAX prototype

April 2020

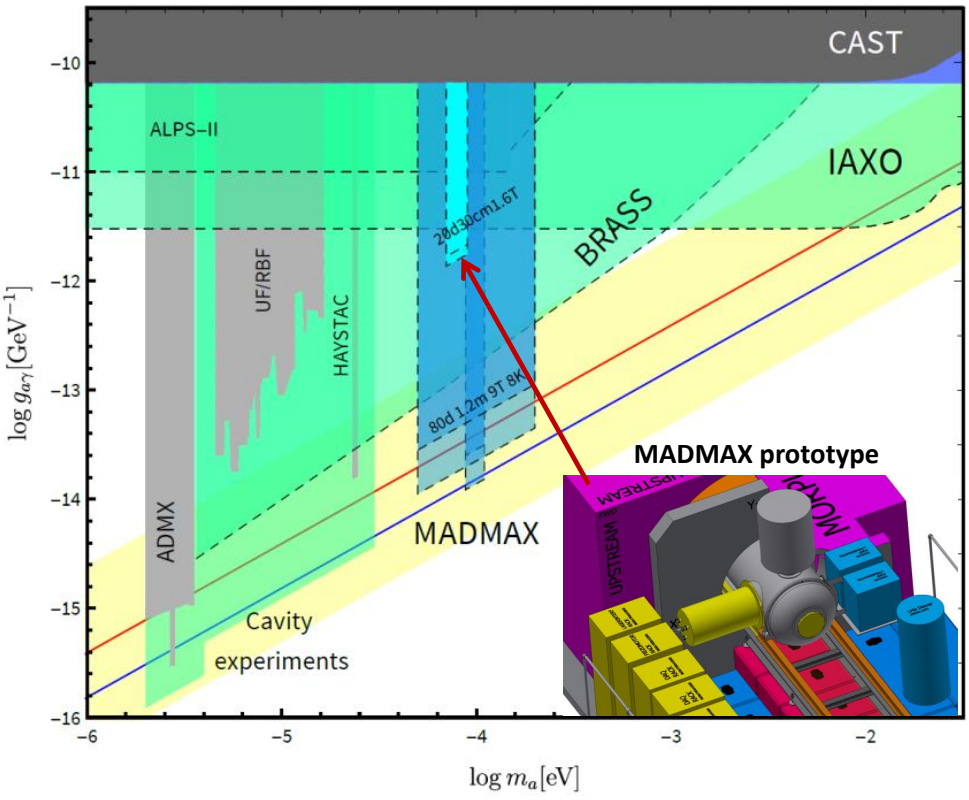

The MADMAX collaboration:

S. Beurthey [f], N. Böhmer [e], P. Brun [h], A. Caldwell [g], L. Chevalier [h], C. Diaconu [f], G. Dvali [g], M. Esposito [c], P. Freire [b], A. Gardikiotis [e], E. Garutti [e], C. Gooch [g], A. Hambarzumjan [g], S. Heyminck [b], F. Hubaut [f], J. Jochum [i], P. Karst [f], S. Khan [i], D. Kittlinger [g], S. Knirck [g], M. Kramer [b], C. Krieger [e], T. Lasserre [h], C. Lee [g], X. Li [g], A. Lindner [d], B. Majorovits [g], M. Matysek [e], S. Martens [e], E. Öz [a], P. Pataguppi [i], L. Planat [c], P. Pralavorio [f], G. Raffelt [g], A. Ranadive [c], J. Redondo [j], O. Reimann [g], A. Ringwald [d], N. Roch [c], K. Saikawa [g], A. Sedlak [g], L. Shtembari [g], F. Steffen [g], C. Strandhagen [i], D. Strom [g], A. Schmidt [a], J. Schütte-Engel [e], J. Schaffran [d], G. Wieching [b]

[a]RWTH Aachen, Germany
[b]Max-Planck-Institut für Radioastronomie Bonn, Germany
[d]DESY, Hamburg, Germany
[e]Universität Hamburg, Hamburg, Germany
[f]Aix Marseille Univ., CNRS/IN2P3, CPPM, Marseille, France
[g]Max-Planck-Institut für Physik, München, Germany
[h]CEA-Irfu Saclay, France
[i]Physikalisches Institut, Eberhard Karls Universität Tübingen, Tübingen, Germany
[j]Universidad Zaragoza, Zaragoza, Spain

Spokesperson: B. Majorovits (*bela@mpp.mpg.de*)
Chair of the collaboration board: E. Garutti (*erika.garutti@desy.de*)
Technical coordinator: P. Karst (*karst@cppm.in2p3.fr*)
Chair of the Physics board: A. Schmidt (*Alexander.Schmidt@physik.rwth-aachen.de*)
MADMAX representative at CERN: P. Pralavorio (*pralavor@cppm.in2p3.fr*)

URL: `http://madmax.mpp.mpg.de/`

Abstract

The MAgnetized Disk and Mirror Axion eXperiment (MADMAX) is a new initiative to search for dark matter axions in the mass range of 40 to 400 μeV. The MADMAX collaboration is presently preparing its prototype booster to validate the experimental concept by proving the mechanical feasibility. Here we propose to use the MORPURGO magnet at CERN during SPS shutdown periods to demonstrate the mechanical feasibility of the concept in an external static B-field. Additionally, the MORPURGO magnet would be used to perform a first competitive search for ALPs in a so far unexplored parameter range.

Contents

1 Executive summary

The axion, originally introduced to solve the strong CP problem, is an excellent dark matter candidate. The dielectric haloscope is a promising technique for dark matter axion detection in the theoretically well motivated mass range of $40 - 400\,\mu$eV. The detection principle is based on the conversion of axions into photons in a strong magnetic field. The interface between vacuum and dielectric materials is used as a conversion surface. The tiny power produced in the conversion is "boosted" by coherent photon emission from multiple dielectric disk surfaces combined with constructive interference effects when placed in front of a mirror. The "booster" concept has already been scrutinized in some detail [1, 2, 3, 4].

The MADMAX project proposes to realize a dielectric haloscope and is divided into phases:

- **Feasibility** of detector components and detector calibration; of magnet procurement; simulation studies including determination of required mechanical precision.
- **Prototype** of down-scaled booster system. Operation of a prototype in MORPURGO magnet at CERN.
- **Intermediate step** Production of intermediate size magnet from first produced coils. Construction and commissioning of the final booster system and receiver. Demonstration of feasibility to reach the QCD axion line.
- **Final experiment** Upgrade of magnet to final size; Axion search scanning of the relevant parameter space.

The feasibility of the booster concept has been experimentally tested using a proof of principle setup [5] and the MADMAX project has been reviewed by the DESY Physical Review Committee in November 2019. The committee noted in its recommendations [6] :

- **Physics**: "The committee enthusiastically endorses the physics goals of the MADMAX proposal, claiming ultimate sensitivity for a very large axion frequency range 10-100 GHz in two phases"; "there are several straightforward models of cosmology that lead to axions in the frequency range targeted by MADMAX to be the dominant contribution to dark matter";
- **Technology**: "The committee is impressed by the ingenuity of this new method to search for axions as dark matter particles in the frequency range of 10-40 GHz (40-160 μeV) in first phase and 40-100 GHz (160-400 μeV) in second phase"; "Despite being well-motivated the targeted mass range is very difficult to reach in other experiments. Therefore, this presents a unique window of opportunity where the MADMAX collaboration is at least several years ahead of potential competitors"
- **Overall**: "Therefore, the MADMAX experiment has significant discovery potential not only for a new particle, but also for discovering a main constituent of dark

matter"; "The detection of axions will open the field of axion astrophysics and provide insight to the formation of galaxies, but also the strong interactions and it will most certainly secure a Nobel Prize for the experiment."

The MADMAX collaboration is presently starting the prototype phase, which will demonstrate the experimental technology in all its aspects, and will provide a prototype booster system that can be scaled to the final experiment.

Here we propose to test the prototype detector and verify the overall concept inside the B-field of the MORPURGO dipole magnet located at CERN EHN1. First comptetitive physics results in terms of Axion Like Particle (ALP) searches are expected.

All required inputs for the conceptual design report for the prototype are expected to be ready in 2020. It is planned to use the MORPURGO magnet for first mechanical tests of sub-components of the prototype during the SPS shutdown Dec. 2021 to March 2022. The prototype will be built and fully commissioned (without an external B-field) at Universität Hamburg and may be available for measurements inside the MORPURGO magnet for the SPS shutdown periods after 2022.

The requirements for operating the MADMAX prototype inside the MORPURGO magnet have been identified and discussed with CERN representatives and are described in this document in some details.

The measurements in the MORPURGO magnet would be an important milestone towards realization of MADMAX and could pave the ground towards detection of axion cold dark matter.

We ask the CERN SPSC to endorse our plans and to support us in setting up the the infrastructural boundary conditions necessary to carry out the planned measurement within the MORPURGO magnet.

2 Motivations for dielectric haloscope

2.1 The case for axions

Searches for a neutron electric dipole moment d_n find $|d_\mathrm{n}| < 2.9 \times 10^{-26} e\,\mathrm{cm}$ [7, 8] with electron charge e. Together with limits on other nuclear electric dipole moments, this implies an absence of charge-parity (CP) violation in the strong interactions at least to a degree that is highly puzzling, in particular, in light of the existing sizable CP violation in the electroweak sector of the standard model (SM) of particle physics. The absence of measurable CP violation is one of the most puzzling features within the SM, also called the strong CP problem.

An elegant solution to this puzzle was proposed by Peccei and Quinn in the year 1977 [9, 10]: By extending the SM with a new global chiral U(1) symmetry—the Peccei–Quinn (PQ) symmetry $\mathrm{U(1)_{PQ}}$—that is broken spontaneously at the PQ scale f_a, a mechanism is introduced, which dynamically suppresses CP violation in the strong interactions. The axion, a emerges as the associated pseudo-Nambu-Goldstone boson [11, 12]. For axions there is a linear relation between the mass m_a and the coupling of axions to photons $\mathrm{g}_{a\gamma\gamma}$ due to the fact that $\mathrm{g}_{a\gamma\gamma}$ is inversely proportional to f_a: $m_a \simeq 5.7\,\mu\mathrm{eV}(10^{12}\,\mathrm{GeV}/f_a)$ [13].

Apart from axions, ALPs – naturally arising from string theory – may also be a viable solution of the dark matter problem. For ALPs there is no evident correlation between their coupling strength to photons $\mathrm{g}_{a\gamma\gamma}$ and the mass m_a. Hence, the parameter space in the $\mathrm{g}_{ALP\gamma\gamma}$ vs. m_{ALP} plane is much less restricted than for axions.

While the original PQ proposal assumed f_a to be at the weak scale, axion searches, astrophysical observations and cosmological arguments point to a very high scale of $f_a \gtrsim 3 \times 10^8\,\mathrm{GeV}$ implying a very small axion mass of $m_a \lesssim 0.02$ eV [14, 15, 16].

Remarkably, the axion is also an excellent cold dark matter (CDM) candidate [17, 18, 19]. The m_a range for which the correct CDM abundance would be provided by the axion depends on the order of two critical events in the past: cosmic inflation and the PQ symmetry breaking.

In the first scenario, PQ symmetry breaking occurred before inflation without any subsequent PQ symmetry restoration. Thereby, the initial value of the axion field in our local universe is unique —up to quantum fluctuations— and is fundamentally unpredictable from first principles. The vacuum realignment mechanism [17, 18, 19] can then provide the complete amount of CDM in the form of cold axions for any value of $f_a \gtrsim 10^{10}\,\mathrm{GeV}$ corresponding to a large possible region of the axion CDM mass of $m_a \lesssim 0.5$ meV. The exact value of the axion CDM mass, however, cannot be theoretically predicted because of the random initial value of the axion field in the observable universe.

In the second scenario, inflation occurred before PQ symmetry breaking. This implies a patchy structure of the axion field in the observable universe with its initial value being essentially random in each patch of the universe causally disconnected during PQ symmetry breaking. The relic axion CDM density from the vacuum realignment mechanism is then given by the statistical average and depends on f_a only [17, 18, 19]. However, the patchy structure is associated with cosmic strings and domain walls which complicates the

calculation of the axion CDM density such that the exact value of the axion CDM mass — i.e. the m_a value for which axions provide the correct CDM density — in this scenario is still the subject of frontier research in astroparticle physics [20, 21, 22, 23, 24, 25, 26, 27]. Currently, the mass range $26\,\mu\text{eV} \lesssim m_a \lesssim 1\,\text{meV}$ is considered as the best motivated one in the post-inflationary PQ-symmetry-breaking scenario with $m_a \sim 100\ \mu\text{eV}$ as a typical representative value for the CDM axion mass [28].

2.2 The dielectric haloscope

The underlying fundamental physics of a dielectric haloscope is described by the modified Maxwell equations [2] (and references therein) obtained when accounting for the Lagrangian density describing axion-photon interactions.

Considering a medium with permeability $\mu = 1$ and a dielectric constant ϵ inside of an external static and homogeneous B-field $\mathbf{B}_\text{e}$, the corresponding modified Maxwell equations imply the existence of a tiny axion-induced electric field

$$\mathbf{E}_a(t) = -\frac{\alpha}{2\pi\epsilon} C_{a\gamma} \mathbf{B}_\text{e} \theta(t), \tag{1}$$

with $C_{a\gamma}$ a model dependent parameter to be expected to be of order 1.

At an interface between media with different ϵ, $\mathbf{E}_a(t)$ is discontinuous, whereas the (modified) Maxwell equations require continuous total $\mathbf{E}$ (and $\mathbf{H}$) field components parallel to the boundary. The continuity is ensured by the emissions of electromagnetic radiation at the boundary in the direction perpendicular to the boundary. The corresponding power output of a single magnetized metallic mirror of area A is [29]

$$P_{\gamma,0} = 2.2 \times 10^{-27}\,\text{W} \left(\frac{A}{1\ \text{m}^2}\right) \left(\frac{B_\text{e}}{10\ \text{T}}\right)^2 \left(\frac{\rho_a}{0.3\ \text{GeV/cm}^3}\right) C_{a\gamma}^2\,, \tag{2}$$

where the ratio of $C_{a\gamma}$ to f_a determines the axion photon coupling $g_{a\gamma} = \frac{\alpha}{2\pi}\frac{C_{a\gamma}}{f_a}$ (α being the fine structure constant) and ρ_a is the galactic local axion CDM density. The MADMAX dielectric haloscope is using movable dielectric discs in front of a metallic mirror exploiting constructive interference and resonant enhancements of the radiation emitted at the many interfaces [1, 2, 30] as sketched in Fig. 1. By optimizing the spacing between the individual discs (each of transverse surface area A), it can be shown that a significant frequency-dependent boost of the power output can be achieved:

$$P_\gamma(\nu) = \beta^2(\nu)\, P_{\gamma,0} = 1.1 \times 10^{-22}\,\text{W} \left(\frac{\beta^2(\nu)}{5\times10^4}\right) \left(\frac{A}{1\,\text{m}^2}\right) \left(\frac{B_\text{e}}{10\,\text{T}}\right)^2 \left(\frac{\rho_a}{0.3\,\text{GeV/cm}^3}\right) C_{a\gamma}^2\,. \tag{3}$$

Here, the enhancement as a function of frequency with respect to a single magnetized mirror is quantified in terms of the power boost factor, $\beta^2(\nu)$, generally referred to as boost factor in the following. It depends on the widths, separations, and on the dielectric constant ϵ of the dielectric discs.

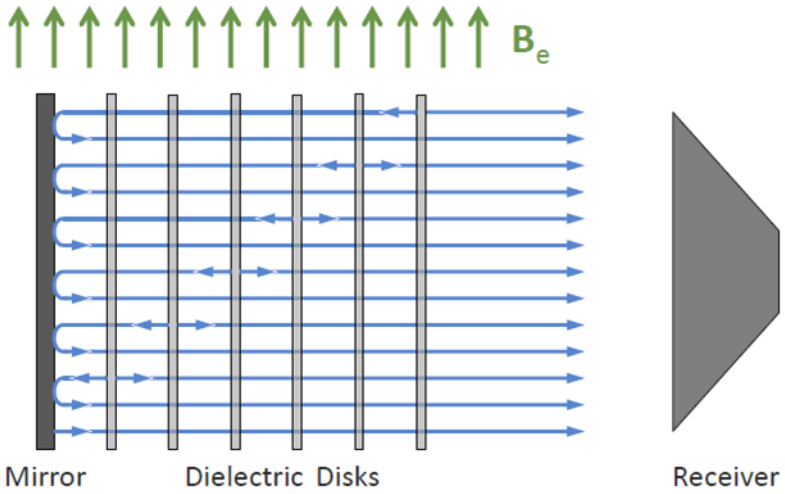

Figure 1: A dielectric haloscope consisting of a mirror and six dielectric discs placed in an external magnetic field $\mathbf{B}_e$ and a receiver in the field-free region. The photon emission (ignoring internal reflections) is sketched by blue lines. A focusing mirror (not shown) could be used to concentrate the emitted power into the receiver. Internal reflections are not shown. From [1].

As an illustration, Fig 2 left shows the boost factor expected for an idealized MADMAX prototype at a frequency of 22 GHz for different analytical calculations (1D, 3D Finite Element Method [31, 32, 33] and 3D Iterative Fourier Propagation). The two 3D methods agree at the percent level giving a β^2 above 10^4 in a bandwidth of 50 MHz.

The power of the axion signal from a booster with $\sim 1\,\mathrm{m}^2$ area and a boost factor $\sim 2 \cdot 10^4$ is expected to be $\sim 10^{-22}\,\mathrm{W}$. In order to detect such a small signal with up to a week of measurement time, a receiver with very low noise is required.

2.3 Sensitivity reach of the dielectric haloscope

With the proposed dielectric haloscope MADMAX it is planned to detect CDM axions if they are in the mass range

$$40\,\mu\mathrm{eV} \lesssim m_a \lesssim 400\,\mu\mathrm{eV}. \tag{4}$$

The existing studies suggest that MADMAX has the potential to cover this important range in the particularly well-motivated axion CDM mass region with a sensitivity expected to reach the most prominent QCD axion models (see Fig. 3).

While the final MADMAX setup should ultimately be sensitive to QCD axion models, there is a significant unexplored parameter range of Axion Like Particles (ALPs) that could explain the CDM in our universe that could be accessible with the down-scaled MADMAX prototype (discussed in section 3.4) inside the MORPURGO magnet.

Fig. 3 shows the parameter region spanned by the axion-ALP mass m_a and the axion-ALP-photon coupling $g_{a\gamma}$ with astrophysical limits (blue), limits from searches (gray),

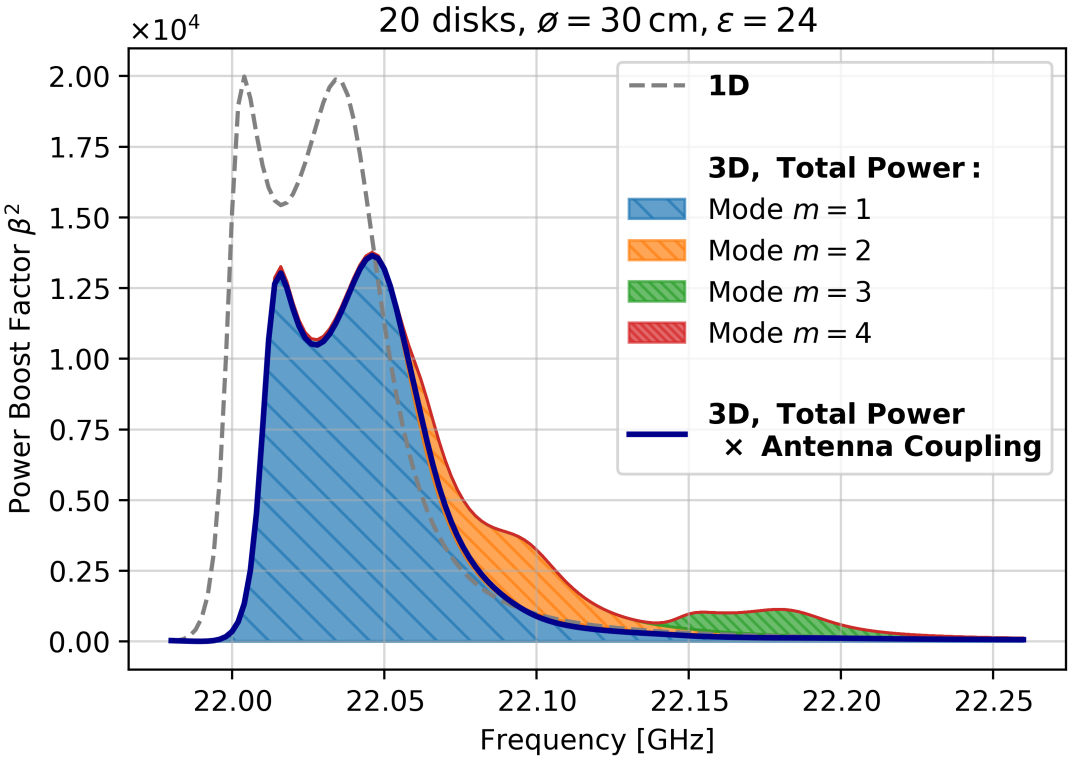

Figure 2: Boost factor considering the finite size of the dielectric discs, tuned to cover a bandwidth of ≈50 MHz at a frequency of ≈22 GHz. Shown are the 1D analytical calculation following [2] (blue line), the 3D total power (orange line) and the power coupled to a Gaussian beam (red line). FEM results (dashed lines), Iterative Fourier Propagation (straight lines) and the contribution from different modes (different colored hatched areas) agree within the percent level, such that the corresponding curves lay on top of each other. A system with 20 discs of 30 cm diameter is considered as in the proposed MADMAX prototype (antenna with a beam waist of 10 cm).

projected sensitivities of planned projects (green) and the location of typical QCD axion models (red and blue lines).

Presently, axion QCD models [34, 35] are tested only by the ongoing ADMX cavity haloscope searches, and by the solar axion search with the helioscope CAST towards relatively large m_a values [36].

The discovery potential of MADMAX shown in Fig. 3 is expected to cover the QCD axion model line for the post inflationary symmetry breaking scenario. Also cavity haloscopes such as CULTASK [37] and the axion helioscope IAXO [38] could reach the sensitivity to detect QCD axions. Also, the discovery reach of the light-shining-through-the-wall experiment ALPS-II [39] and the magnetized dish antenna experiment BRASS [40] are shown in Fig. 3.

The sensitivity of the MADMAX project and the period needed to scan the full mass

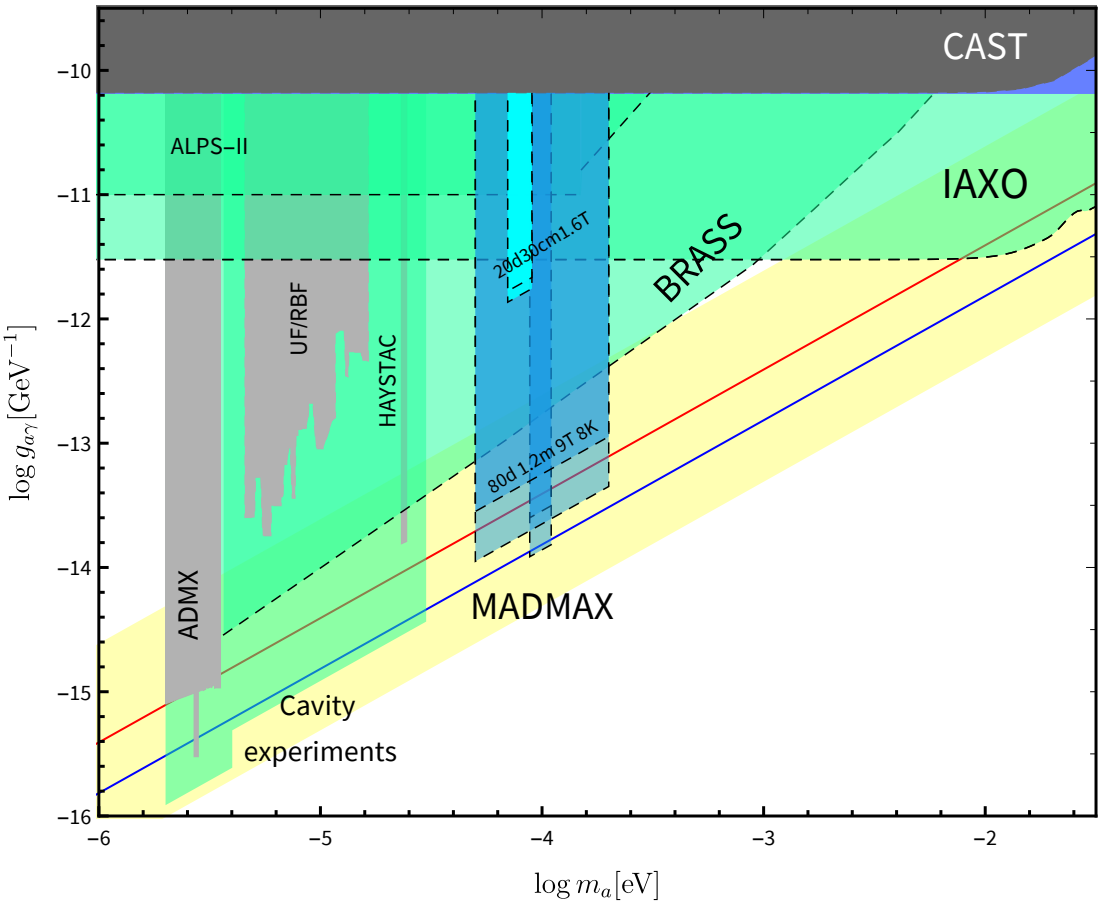

Figure 3: Sensitivity of MADMAX shown in the parameter region spanned by the axion/ALP mass m_a and the axion/ALP-photon coupling $g_{a\gamma}$. The diagonal red and blue lines indicate the location of two prominent QCD axion models (KSVZ and DFZS, respectively). The yellow area displays the range of plausible models for the ratio $\mathcal{E}/\mathcal{N}$ [41]. Astrophysical limits (blue) and limits from searches (gray) with cavity haloscopes (ADMX, HAYSTAC, UF/RBF [42, 43]) and the axion helioscope CAST are shown. The expected sensitivity of future cavity experiments (e.g. ADMX, HAYSTAC, CULTASK), the axion helioscope IAXO, the light-shining-through-the-wall experiment ALPS-II and the magnetized dish antenna haloscope BRASS are also indicated. The sensitivity range for MADMAX is shown for two cases (blue regions): a wide- and a narrow-mass-range scan. For both cases the sensitivity is shown for a "conservative" and a more "success oriented" set of parameters (see text). Also the projected sensitivity for the prototype with 20 discs in a 1.6 T field at 8K within 90 days measurement time is shown in cyan (see Sec. 3.4). MADMAX sensitivities correspond to $5\,\sigma$ signal above noise. The other limits and sensitivities may have other definitions.

range depends on the assumptions on achievable boost factor (loss effects), achievable noise temperature of the receiver ($T_{\rm sys}$), coupling of the antenna-receiver system to the booster and the readjustment time (t_R) for the disc positions between measurements at

Full members	Acronym
RWTH Aachen, Germany	RWTH
Max-Planck-Institut für Radioastronomie Bonn, Germany	MPIfR
DESY Hamburg, Germany	DESY
Universität Hamburg, Germany	UHH
Centre de Physique des Particules de Marseille, France	CPPM
Max-Planck-Institut für Physik, München, Germany	MPP
CEA-Irfu Saclay, France	CEA
Eberhard-Karls-Universität Tübingen, Germany	Uni. Tübingen
Universidad Zaragoza, Spain	Uni. Zaragoza
Associate members	
Institut NEEL, CNRS, Grenoble, France	NEEL

Table 1: List of MADMAX member institutions

different mass-ranges. The depicted sensitivity reach of MADMAX is defined as a signal with $5\,\sigma$ above system noise temperature. It is assumed that 50 % of the theoretically obtainable maximum power is detected (30% loss from 3D effects, and another 30% from antenna coupling). The reach of MADMAX is shown for a wide- and a narrow-mass-range scan, each of them under two sets of assumptions: "conservative" (upper dashed line) and "success oriented" (lower dashed line). The conservative set assumes boost-factor bandwidth $\Delta\nu_\beta = 50$ MHz, $t_R = 1$ day, $T_{\rm sys} = 8$ K and a live time of 3 years. The success oriented assumes $\Delta\nu_\beta = 20$ MHz, $t_R = 1$h, $T_{\rm sys} = 4$ K and 5 years scanning time.

3 The MADMAX dielectric haloscope

3.1 Collaboration

The MADMAX collaboration was founded at DESY-Hamburg in October 2017. Currently, it consists of nine institutes as full members and one associate members. The member institutes are listed in Tab. 1.

3.2 Experimental concept

The MADMAX project is based on the idea of the dielectric haloscope: the axion induced power output of a single dielectric surface is boosted by the system to $\approx 10^{-22}$ W, cf. eq. (3). This could be realistically measured with high enough significance within a $\sim$ week of integration time with an overall noise temperature of 8 K. To obtain this power, a power boost $\beta^2 \gtrsim 2 \times 10^4$ and a dipole magnet with a figure of merit

$$\mathrm{FoM} = \frac{1}{L}\int_A \int_0^L B(x,y,z)^2 dz dx dy \approx 100\ \mathrm{T}^2\mathrm{m}^2, \tag{5}$$

are aimed for. Here $B(x, y, z)$ gives the y-component of the B-field as a function of the position, L is the maximum length of the booster[1] and, A is the area of each disc contributing to the axion to photon conversion.

The planned MADMAX experiment would consist of the following main components:

- **Magnet**: A $\approx 9\,\mathrm{T}$ dipole magnet with a 1.35 m warm bore out of which the inner 1.25 m should be available for the disc areas to get FoM $=100\,\mathrm{T}^2\mathrm{m}^2$;
- **Booster**: The booster including up to 80 dielectric discs in front of a mirror with $\approx 1.2\,\mathrm{m}^2$ area, adjustable in their relative distance between 1.5 and 15 mm with a precision of better than $\sim 10\ \mu$m;
- **Optical system and receiver**: The axion induced radiation emitted by the booster is guided and focused onto the receiver by the optical system. It consists of the horn antenna and focusing mirror. An exchangeable receiver to enable the detection of signal photons in the frequency range of 10-100 GHz is coupled to the optical system.

A design concept for a dipole magnet with the required aperture and FoM already exists. It is planned to first build an intermediate scale magnet out of the first available coils for integrity tests. This first step magnet could also prove the principle feasibility of reaching the sensitivity to scan the QCD axion line. These efforts are independent of the efforts about constructing and operating the prototype in the MORPURGO magnet.

The booster consists of a fixed copper mirror and the dielectric discs, both with diameter 1.25 m, the construction that keeps in place and moves the discs, and a system that allows to obtain the real-time position of the discs. It has to be operated at liquid helium temperature inside a high B-field, with a disc positioning accuracy of a few μm. The maximum disc displacement could be up to 1.2 m (difference of disc position for the two extreme frequencies 10 GHz and 100 GHz with 80 discs). There is no off-the-shelf solution for this long stroke positioning in a cryogenic environment. For several parts of the booster system, significant developments are required to meet these goals.

The booster and optical system will be situated in a liquid helium cooled cryostat, in order to reduce the system noise temperature.

The receiver will be attached to the booster cryostat. A conceptual sketch of such a system (without the receiver cryostat) is shown in Fig. 4.

The prototype that is going to be built for verification of the concept can be subdivided into the same components.

3.3 Proof of principle tests and validation through simulations

The experimental concept has been investigated using a proof of principle setup with reduced number of discs of smaller size (20 cm diameter). The setup has been characterized using reflectivity measurements. The group delay, obtained from these measurements can be related to the boost factor of the measured booster system. Therefore, investigation of

[1] The z-axis points along the axis of the cylindrical booster. The y-axis is vertical.

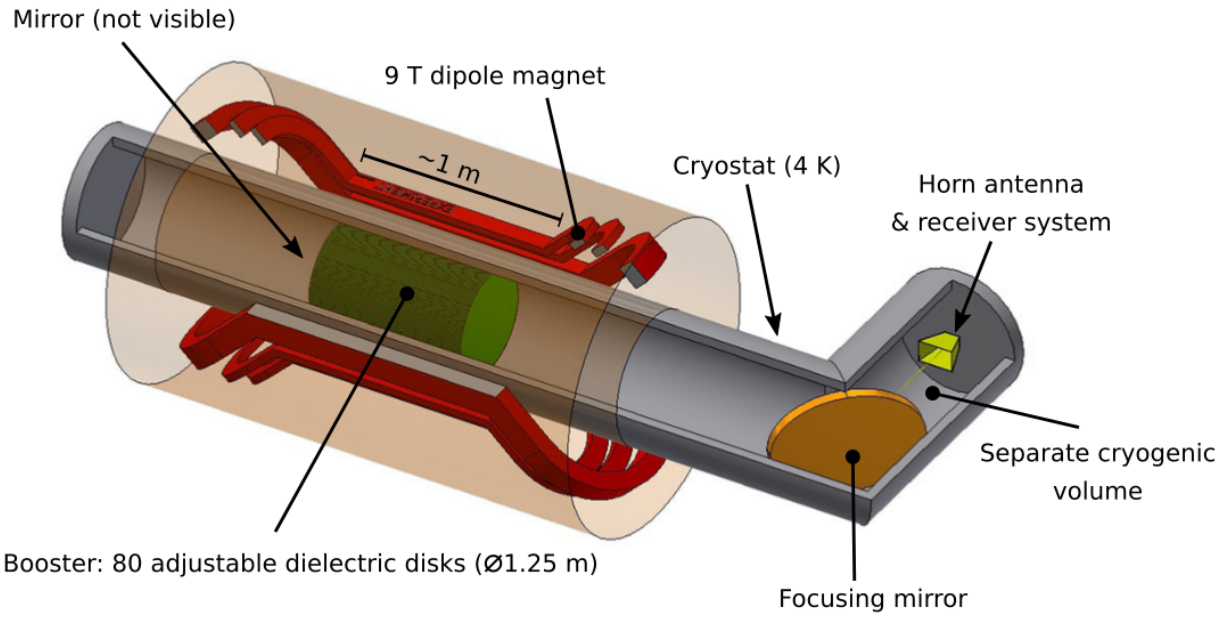

Figure 4: Conceptual sketch of the MADMAX experiment (taken from [44]).

the reproducibility of reflectivity can give information on the effect of inaccuracies of the system on the boost factor itself

Several measurements have been performed with up to five discs (Fig. 5) that confirm some of the basic assumptions made [5]:

- An individual disc can be placed with a reproducibilty of the order μm,
- the main group delay peak of the system is reproducible with accuracy of $\sim 1\,$MHz,
- individual disc positions are reproducible with μm precision,
- first order reflections from the antenna mismatch can be modelled into the booster response,
- stability of 1D boost factor to 1 MHz,
- stability of obtainable boost factor within a few percent,
- time needed for positioning algorithm approximately linear with number of discs.

For the receiver at frequencies below $\sim$ 40 GHz, there exists a mature technology – the High Electron Mobility Transistor (HEMT) based amplifier – that has a noise temperature of a few Kelvin when operated at liquid helium temperature. It has been demonstrated in the lab that the aforementioned receiver chain is capable of detecting signals of 10^{-22} W within a few days. A linear detection scheme based on heterodyne mixing is typically

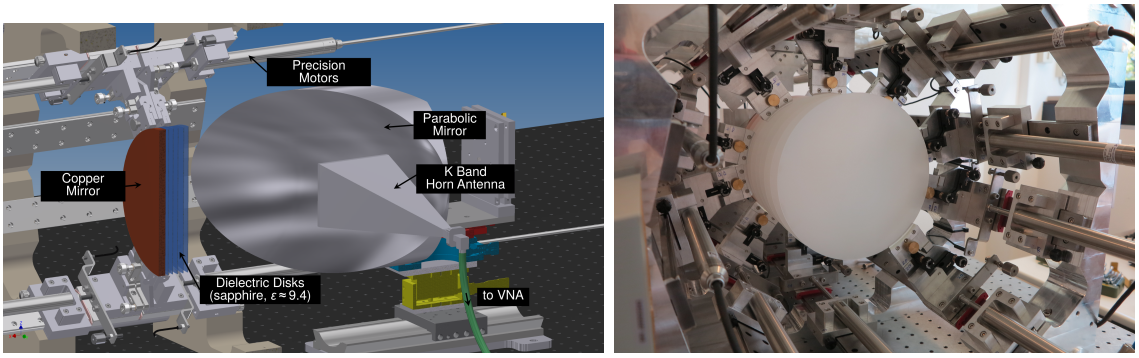

Figure 5: Left: Sketch of the proof of principle experimental setup used for reflectivity measurements. Right: Picture of the proof of principle setup with sapphire discs installed.

used, whereby the signal to noise ratio (SNR) is given by Dicke's radiometer equation,

$$\mathrm{SNR} = \frac{P_{sig}}{k_B T_{sys}} \sqrt{\frac{t_{scan}}{\Delta\nu}}. \tag{6}$$

where k_B is the Boltzmann constant, P_{sig} is the expected axion signal power corrected by detection efficiency. T_{sys} is the total system noise temperature which consists of the receiver noise temperature T_R and the additional noise from the booster and its surroundings $T_{booster}$, such that $T_{sys} = T_R + T_{booster}$. $\Delta\nu = 10^{-6}\nu_a$ is given by the axion line width and t_{scan} is the integration time for an individual measurement of a given bandwidth.

Measurements have been performed with the proof-of-principle receiver chain in which a "fake axion" signal at 18.4 GHz with power of $\sim 1.2 \times 10^{-22}$ W [2] and could be detected [45] with two days of measurement time with a significance of $\gtrsim 4.8\sigma$.

Simulations using different methods (different finite element calculations, recursive Fourier transformation, etc.) have been performed to study the susceptibility of the boost factor to 3D inaccuracies of the system like tilt of the discs, surface roughness, inhomogeneity of dielectric constant, inaccuracies of disc positioning, disc tiling or axion velocity distribution. The investigations show that using realistic assumptions a boost factor exceeding 10^4 should still be possible. The main implications for the final setup with 80 discs and 1.2m disc diameter are given by the following parameter:

- Dielectric loss of discs $\lesssim 10^{-4}$.
- Motor positioning uncertainty $\lesssim 3$ μm.
- Surface roughness of the discs better than 20 μm at a correlation length of $\lambda/4$, corresponding to ~ 4 mm at ~ 20 GHz.
- Planarity of the discs better than $\sim$ few μm at a correlation length of 35 mm.
- Tilts of discs lower than ~ 0.1 mrad,

[2] The "fake axion" signal is injected directly into the receiver without going through an antenna.

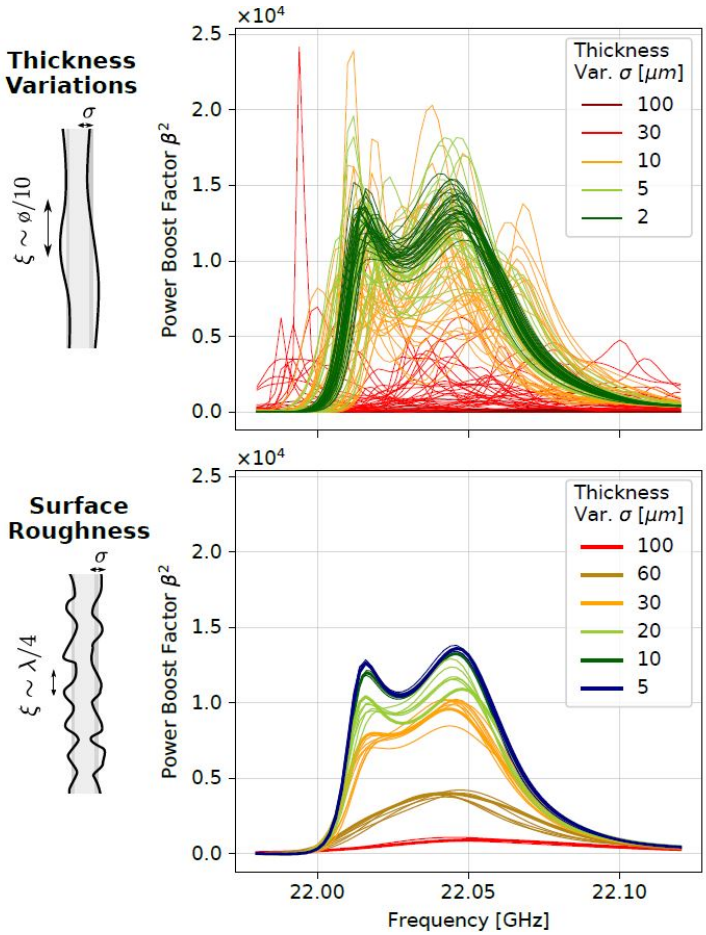

Figure 6: Results for simulations with different assumptions on the thickness variations (top) and surface roughness (bottom) for the prototype setup. Different colors correspond to different roughness, different boost factor curves in same color correspond to different simulations with same assumption on the mean surface roughness. (adapted from [46])

- Magnet inhomogeneity in direction of booster length (B-field gradient) better than 30% (Note that this number is minimized in order to maximize the FoM eq. 5).

- Axion velocity $\lesssim 0.01\,\mathrm{c}$.

As an example Fig. 6 shows the results for simulations with different assumptions on the disc thickness roughness for the final setup with 20 discs made of $LaAlO_3$ and diameter of 30 cm. Each assumption for disc roughness has been simulated repeatedly, corresponding to individual lines with same colors. Different colors correspond different assumptions for variation of the surface roughness or planarity.

A design study was performed by a company experienced in cryogenic engineering and

drive concepts for cryogenic environment, JPE [47, 48][3]. The study aimed at identifying a mechanical concepts for precise movement of the booster discs inside the final booster setup given the boundary conditions of the experiment. It was concluded that a booster could be built for operation at 4 K with carriages for the discs fixed on rails. The carriages would have piezo elements integrated into them that allow to move them along the rail. A first prototype carriage rail system is presently under construction an will soon be tested in cryogenic surrounding.

The dielectric discs have to be made from material with low dielectric loss and high dielectric constant. Single crystal sapphire ($\epsilon \sim 9$, $\tan\delta \sim 10^{-5}$) and $LaAlO_3$ ($\epsilon \sim 24$, $\tan\delta \lesssim 10^{-4}$) have been identified as good candidate materials. Single crystals with the needed quality are available only with size smaller than the required disc. Therefore, discs need to be tiled.

3.4 Prototyping MADMAX

For verification of the experimental feasibility it is essential to start with a down scaled version. It needs to be demonstrated that such a system can be built and operated under the boundary conditions expected in the final setup (cryogenic temperature, high B-field). For this a prototype system is being deigned and built.

The MADMAX prototype is a down-scaled version of the final experiment with the specific task of testing all technological components of MADMAX, establishing the data taking procedure and potentially acquiring the first physics results on ALPs and hidden photon searches with this technology.

The down-scaling is by a factor of 1/10 in area of the discs, 1/4 in the number of discs and 1/6 in the magnetic field strength. It has the same structure and components as the final booster but reduced overall size. The cryogenic vessel containing the prototype booster and the optical system is being designed to fit the open bore of the MORPURGO magnet at CERN. The prototype design is flexible enough to account for changes in the booster design to accommodate for the shortcomings identified during commissioning. The feed-through to the receiver is also kept flexible to offer the possibility of testing various receiver concepts. A CAD implementation of the prototype is shown in in Fig. 7.

3.4.1 Prototype booster design

The booster structure will support 20 discs of 30 cm diameter, the motors necessary to move them and the system to control the motors. It will provide the sufficient rigidity to obtain the required alignment tolerance of the discs. The CAD drawings for the final booster received from JPE have been down-scaled to a 20 disc system and are presently being finalized. Final production drawings for the prototype booster should be available mid-2020. The current design of the prototype booster is shown in Fig. 8.

[3] https://www.janssenprecisionengineering.com/

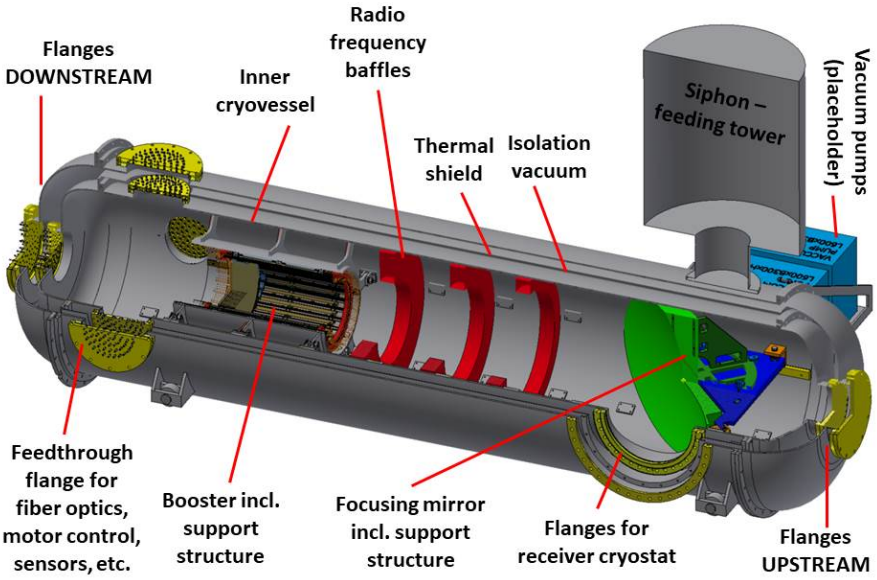

Figure 7: CAD implementation of the MADMAX prototype cryostat. The two vacuum pumps attached to the cryostat are also shown.

3.4.2 Dielectric disc tiling

Tiling of 30 cm discs using a refurbished CNC (computer numerical control) machining tool has already been demonstrated, even if the requirements for planarity could not yet be reached. The development of the tiling procedure and disc characterization to the needed accuracy is ongoing work.

3.4.3 Real time disc position measurement

For the real time distance measurement of the disc positions needed to align the discs properly with respect to the copper mirror it is planned to use interferometer measurements at three positions 120^o apart at the circumference of each disc. For the required accuracy in the harsh environment, only optical measurements seem feasible. A precision laser interferometer from the company HighFinesse[4] seems to be a viable solution: it provides an absolute measurement of the disc position with accuracy below 1 μm, allowing to determine the tilt of the discs with sufficient accuracy if three points per discs are measured. The system can provide real-time feedback at a rate of 10 Hz. Such a system has been already tested inside a mockup with a copper mirror and two discs. Tilts could be measured with a reproducibilty of 0.1 mrad.

[4]https://www.highfinesse.com/en/

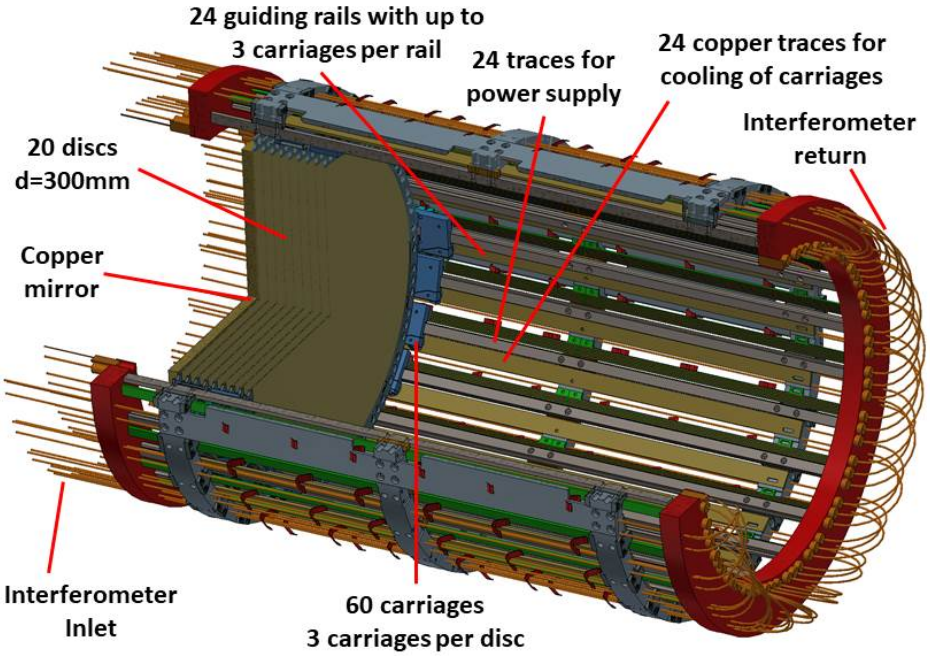

Figure 8: Design of the prototype booster

3.4.4 Optical system

A simplified sketch of optical system of the MADMAX prototype, consisting of an elliptical focusing mirror and horn antenna is shown in Fig 9. The size of the focusing mirror for the prototype, sitting at a distance of $\sim$2 m behind the booster, has been optimized for the ideal coupling of the Gaussian beam shape into the horn antenna. Its size is related to the expected beam waist of the booster signal. This was determined from simulations. This leads to a diameter of the focusing mirror of ~ 1 m, which determines the inner diameter of the cryostat (~ 0.7 m, as the elliptical focusing mirror is placed diagonally). The coupling integral to the Gaussian beam (first mode) is $> 95\%$ in the frequency range between 18 and 25 GHz.

Additionally, the cryostat walls will be equipped with radio frequency baffles as absorber elements to minimize radiation of reflected signals towards the receiver. In order to assure proper alignment between booster system even after cool down from room temperature to 4 K, the focusing mirror and the horn antenna will be suspended in a way to allow for shrinkage along the proper axes.

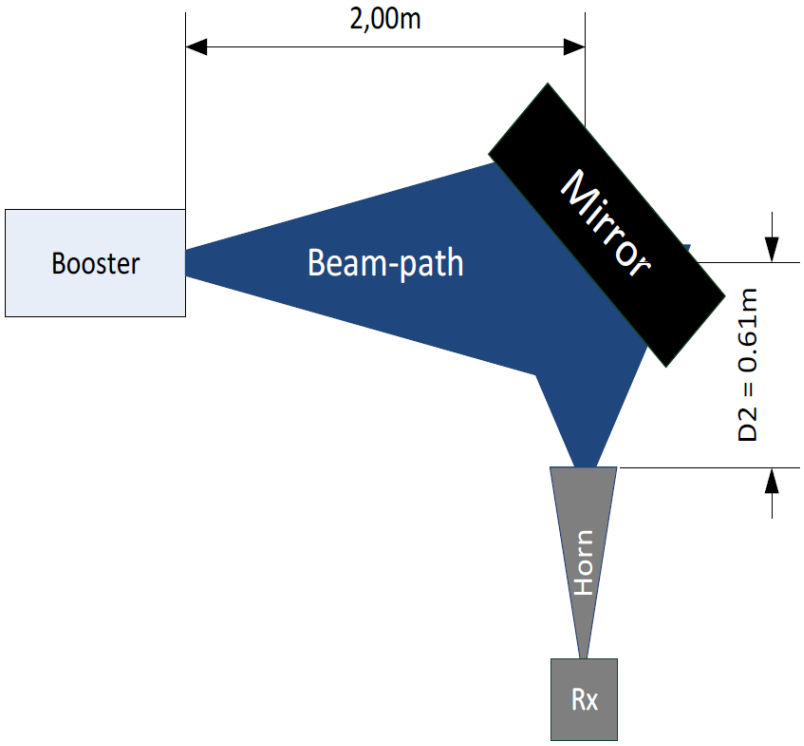

Figure 9: Simplified sketch of the MADMAX optical system collecting and guiding the signal from the prototype booster to the receiver system.

3.4.5 The cryostat vessel

The prototype cryostat will have an inner diameter of 750 mm determined by the size of the focusing mirror. The outer diameter is limited by the constraints of the MORPURGO magnet at CERN and the foreseen place for commissioning of the whole prototype system, the SHELL laboratory at the university of Hamburg. The cryostat vessel also includes the various interfaces (flanges) to the subsystems of the prototype, e.g. the prototype booster and the laser interferometer as well as the focusing mirror (see Fig. 7). These interfaces include electrical and optical feed-throughs as well as thermal couplings.

Cooling of the cryostat and the components sitting inside during operation will be provided with a feeding tower containing a Liquid Helium (LHe) reservoir. The LHe flow in the closed circuit is driven by gravity and the evaporated helium flowing back to the tower. The helium gas will be reliquified by up to five vibrationally de-coupled cryo-coolers. The baseline design foresees cooling of the thermal shield by the evaporated cold helium gas, where the required flow will be generated by a pump (either a cold pump or a warm pump in combination with a counterflow heat exchanger) and the gas is recooled at the first stage of the cryocoolers.

The estimated ~ 6 W of heat losses require a helium re-liquefaction rate of roughly 200 l per day. The cooling water for the compressors (needed for the cryo coolers) and the

max. length with end-flanges dismounted	mm	3500
max. length incl. end-flanges	mm	4250
max. diameter Diameter (incl. flanges, no feedthroughs)	mm	1200
max. width including receiver and pumps	mm	3100
max. weight including all components	kg	5000
Estimated cool down time	days	14
Cool down LHe consumption	l	~ 2500
Amount of LHe in system during operation	l	50 – 100
LN consumption cool-down	l	~ 1500
Heat losses at 4.5K	W	~ 5
Power consumption during operation (cryo coolers)	kW	~ 90
Max. exhaust helium gas	l/s	tbd.

Table 2: Main characteristics of the MADMAX prototype cryostat.

(warm) pump are provided by a water chiller.

Two pumping stations, attached to the cryostat, will be needed for evacuation of the independent insulation and cryostat booster vacua.

Cooling down of the cryostat from room temperature will happen via supply of cryogenic liquids through transport dewars. It is estimated that in total 1500 l of liquid nitrogen (LN) will be necessary for pre-cooling to 77 K and 2500 l of lHe to cool the inner cryostat to 4.2 K, assuming a cold mass of ~ 1 t.

During design great care is being taken to comply with all applicable European Directives regulating safety aspects, specifically Council Directives 2006/95/EC (Low Voltage Directive), 98/37/EC (Machinery Directive - 2006/42/EG after 01/01/2009), 89/336/EEC (Electromagnetic Compatibility Directive - 2004/108/EC after 20/07/2009) and 2014/68/EU (Pressure Equipment Directive, PED). It is planned to forward the detailed design to CERN expert as soon as the drawings are available. Already before this, MADMAX representatives will be in close contact with the CERN experts in order to clarify the main requirements with respect to safety and other regulations.

Table 2 gives the main characteristics of the cryostat relevant for operation at CERN.

3.4.6 The receiver

In a first step, commercially available HEMTs with a noise temperature of ~ 5K - if operated at physical temperatures $\lesssim 8$K - will be used. They easily fit into the same cryostat extension as necessary for the horn antenna. In a second step it is planned to use travelling wave parametric amplifiers (TWPAs), which need to be operated at ~ 100 mK. For this second step a dilution refrigerator will be needed that can be coupled to the cryostat (note that the dilution refrigerator has not been considered in the estimated power consumption).

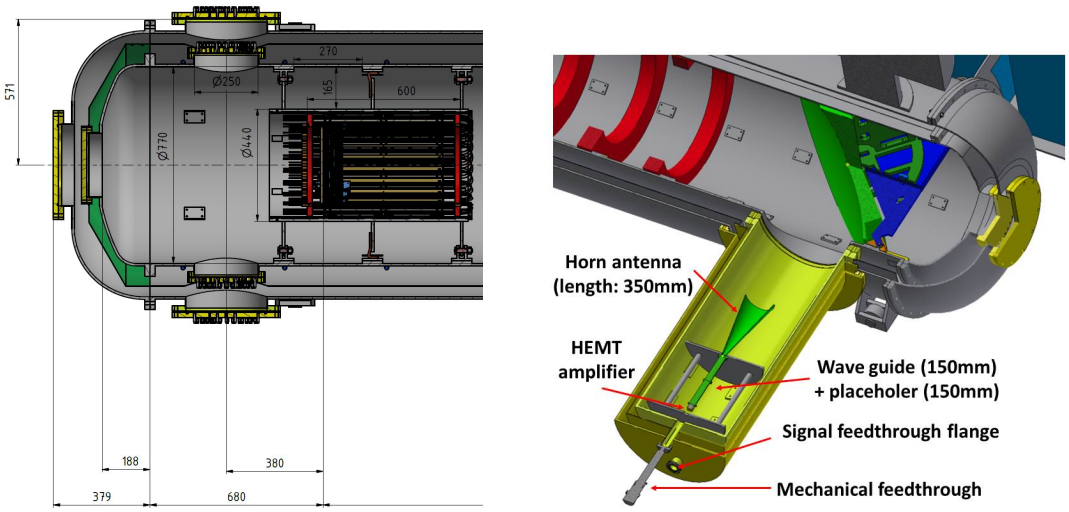

Figure 10: Detailed view of the cryotat vessel including the booster, the focusing mirror and the receiver cryostat.

3.4.7 Feedthroughs

A sketch of feedthroughs of the cryostat vessel for piezo motor control and the interferometer device as well as the part containing the cryostat receiver can is shown in Fig. 10.

4 Technological challenges and the role of CERN

The MADMAX project includes several technological challenges.

- Magnet: Building of a large aperture strong B-field dipole magnet
- Determination of the boost factor: Verification of the simulation and calibration strategy
- Disc displacement system: Operation of displacement system at cryogenic temperatures inside strong B-field with necessary accuracy.
- Disc size and tiling: Production of discs with necessary size and accuracy and operation of these in the required surrounding (cryogenic temperature, strong B-field)
- Detection technology: Implementation of low noise detection system into the overall system given all boundary conditions.

Except for the magnet itself, these will all – at least partially – be addressed by the scaled-down prototype version of the final experiment. Many of the tests need to be performed with the prototype inside an external magnetic field. The output of the tests will be essential for scaling up for the final design of the MADMAX experiment.

The tests inside the MORPURGO magnet at CERN will play a decisive and critical role in helping the final MADMAX experiment to become reality.

Magnet	ALPs test	MORPURGO	GOLIATH	WISP-MAG
Location	DESY hall west	CERN north area		Uni. Hamburg
Magnet type	Dipole	Dipole	Helmholtz	Solenoid
B_{max} [T]	5.7	1.6 (1.9)	1.5	14
Usable aperture [m]	0.055	1.45	2.00	0.150
Usable length [m]	8.8	~ 1	~ 1	0.01
Availability	> 2020	SPS shutdowns		$> 06/2020$
Access	4 K cold bore	warm bore		warm bore
Sample preparation	~ 3 days	-		-
Max dB/dt [T/s]	25	< 0.1	unknown	t.b.c.

Table 3: List of available magnets for testing prototype and individual components

4.1 Measurements inside magnetic field

It is essential to study the behavior of the individual mechanical components inside a strong magnetic field. Measurements are foreseen in different magnets available at DESY Hamburg, University of Hamburg and at CERN. The important parameters of the available magnets are listed in Tab. 3. Two magnets with small usable aperture will be available in Hamburg for testing of individual components like the motors, dielectric materials, etc.

For testing the full prototype the CERN MORPURGO dipole magnet [49] has been identified as an ideal site. Except for the warm bore aperture the main criterion for selection of the magnet is the reachable B-field, which for MORPURGO is 1.6 T, potentially 1.9 T after a possible upgrade. Furthermore the fringe field in the surrounding has to be considered, as pumps and other equipment have to be operated nearby.

Additionally to the MORPURGO magnet, recently the CERN GOLIATH magnet [50] with a B-field of up to 1.5 T has also been proposed as an alternative to host the MADMAX prototype. In order to evaluate feasibility of this magnet for the tests more investigations would need to be performed. Especially the fringe field would need to be studied in more detail.

The MORPURGO magnet is clearly favored for the possibility of achieving a higher magnetic field, also since there might be an option to operate it at 1.9 T. The higher B-field has a significant effect on the results of the campaign, as the forces exerted on the system scale with B^2. The figure of merit for MORPURGO, with a 1.9 T B-field is a factor of 22 lower than the one of the final MADMAX magnet, a factor of 31 for MORPURGO with 1.6 T and a factor of 36 for GOLIATH. The same argument also holds for the sensitivity for ALPs.

The MORPURGO magnet could be available during the SPS shutdowns each year from December to April starting from December 2021. It has an aperture of 1.6 m and 1.45 m is usable once the rails, needed to slide the cryostat, will be installed. Homogeneity of the field is better than 5% in the center of the magnet which fits our requirements for the prototype tests. After clarification of the feasibility with CERN representatives, a letter of intent to the SPSC for the usage of the magnet had been handed in [51].

4.2 Physics measurements in the MORPURGO magnet

Provided that the tests in the magnetic field of MORPURGO are successful and a reliable understanding of the booster optical behavior can be achieved, it is planned to use the prototype inside MORPURGO to produce first competitive limits for ALPs in the mass range around $\approx 100\,\mu$eV as shown in cyan in Fig. 3. A sensitivity to the ALPs photon coupling ($5\,\sigma$ signal above system noise) down to $\approx 10^{-12}$ GeV^{-1} over a mass range of ≈ 5 μeV can be achieved using the following assumptions: a sensitivity of the receiver as described in section 3.4, i.e. a system noise temperature of T_{sys} $\approx 8\,$K; a coupling efficiency between the axion field and the receiver 50 % as compared to the 1D calculations (loss effects, antenna coupling); a readjustment time of the booster discs between different optimized scanning ranges of 1 hour; and a scanning time of 90 days; smallest achievable boost-factor bandwidth of 50 and 20 MHz (upper and lower line, respectively).

5 MADMAX prototype operation at CERN

This section describes the requirements for a smooth operation of the MADMAX prototype in the CERN MORPURGO magnet during the shutdowns in term of infrastructure, cryogenics, electrical connection and floor map around the magnet. This section ends with a tentative planning of operation and time schedule of the prototype. It is worth to note that in parallel with the SPSC process, lots of fruitful discussions took place with the CERN experts (cryogenics, North area, ...) as well as with the ATLAS test beam coordinator. The requirements discussed in this section have already integrated the outcome of these discussions.

5.1 Cleaning of the MORPURGO area

Figure 11 left shows the MORPURGO area as seen from the upstream side. The rails allow the ATLAS pixel and SCT detectors located on the trolley to be inserted in the magnet.

Several changes are needed in order to install and test the prototype inside the magnet. First, the existing rails will have to be dismounted and an independent rail structure installed. These new rails will go through the magnet bore and be supported from both sides of the platform floor [5] to avoid connection with the magnet. Second, the cable tray currently attached to the magnet (Figure 11 right) will need to be removed to allow a complete insertion of the prototype cryostat into the magnet. More generally, suitable experimental conditions including good access to site (cleared access routes, stairs to access the upstream and downstream platforms,..) will be needed. For the installation of the prototype, the available cranes (hooks for 10 t and 40 t) fit our needs.

[5] The original rails can be easily remounted and realigned after the prototype run.

Figure 11: Left) View of the area around the MORPURGO magnet in the north area, as seen from the upstream side. The yoke of the magnet is in red. ATLAS rails are fixed on a support IPN (yellow) and on the magnet. Right) Zoom on the cables attached to the MORPURGO magnet.

5.2 Cryogenics requirements

5.2.1 Vacuum pumps

In total, two pump units are required to operate the cryostat insulation vacuum and the booster/receiver vacuum. To maintain the effective pumping speed, the pumping units will be fixed on the cryostat outer shell and will move with the cryostat. They can be operated only if the ambient magnetic field is below 2 mT. To make sure that this is the case, a simulation of the fringe field around the magnet has been performed, based on the MORPURGO data field map available [52]. This simulation is able to reproduce the available measurements and predicts a field strength below 2 mT on the external vertical wall of the yoke. This corresponds to the location of the pumps when the cryostat will be in position in the magnet.

5.2.2 Nitrogen and Helium consumption

The Liquid Helium needed for cooling down the cryostat can be delivered by CERN cryoLab in 500 l dewars. Approximately five dewars will be needed in total. Exhaust/Recovery line for gaseous helium will be installed. The maximum evaporation rate will occur during cool-down of booster and receiver cryostat and still need to be determined.

Liquid nitrogen dewars have to be provided via an external company that fill the dewar on request – 1500 l is the present estimation for pre-cooling requirement.

5.2.3 Equipment for standard cryogenic operation

The five compressor units and the warm pump have a footprint of 0.5x0.5 m^2 each and will be installed below the upstream platform. One water chiller with a footprint of 1.7×1

m^2, will be installed close-by. It will deliver a cooling power equivalent to a cooling water flow of 4-5 m^3/hour. Additionally, a circulation pump for maintain the helium gas flow of the thermal shield circuit is needed. All the cryogenic equipment will be monitored by a control system rack located nearby the water chiller unit.

5.3 EM noise measurement

Short term measurements in the high frequency regime (10 to 26 GHz) were performed in March 2019. No signals could be detected. These measurements show that the EM background, as determined in the measurement period, is acceptable for measurement with the planned prototype booster setup [51].

5.4 Electric (and grounding) requirements

Five individual racks of electronics will be needed to monitor the DAQ+receiver and the booster (motors, sensors, interferometer, etc.). One additional rack will be needed for monitoring the cryogenic system, including dilution unit (pumps, valves, sensors, etc). Part of these racks will need to be connected to a UPS. This UPS will filter any potentially noisy power. The only requirement regarding "clean power" is that the supply of power should be reliable with no power cuts > 10 minutes.

An equipotential panel will be needed. The panel should be accessible from both sides of the magnet. On the upstream side, the equipotential panel should extend further towards the DAQ (≈ 1 m, see floor plan). The potential difference on the equipotential panel between the two sides should be less than 1V. Two dedicated grounds (one for DAQ, one for interferometer) will be needed. These should be close but NOT connected to the equipotential panel. In order to understand the potential influence from emitters of EM radiation nearby the setup a plan of all electrical installations in the close surrounding (≈ 20m) would be required.

Stable ground at the site is needed with no induction currents in floating surfaces, clean surrounding, damping of vibrations (due to crane movements, etc.).

All the electrical needs are summarized in Table 4. In total about 7 outlets of 400V / 32A and 16 plugs of 230V are required for a total power of 100 kW and 17 kW, respectively.

5.5 Floor map

As can be seen in Figure 11, a large area is available for hosting the MADMAX prototype. Independently of this proposal, this area will be refurbished during the LS2 – especially part of the wall visible in Figure 11 will be dismounted together with the clean rooms located behind. We propose in Figure 12 a floor map that could fit in the 14.4×4.8 m^2 space that was planned to be available. This area will be covered by a large enough clean room tent (including ventilation or climatization required for the electronics) with a dismountable roof, that could be split in two parts, close (Working Space 2 [WS2] with a footprint of 8.4×5.4 m^2) and far (Working Space 1 [WS1] with a footprint of 6×3.8 m^2)

Unit	Number	Power (kW)	Sockets	UPS
Cryogenics				
Compressor for cryocooler	5	5×12=60	5× 400V /32A	No
Warm pump (gHe circulation)	1	10	400V / 32A	No
Water chiller	1	15	400V / 32A	No
Vacuum pumps (insulation/booster)	2	1	230 V	No
Control system	1	1	230 V	Yes
WorkingSpace 1				
DAQ racks	3	3×1=3	230 V	Yes
Piezo-motor rack	1	5	230 V	No
Interferometer rack	1	0.01	230 V	Yes
Oscillators	1	1	230 V	No
WorkingSpace 2				
Equipment	1	1	230 V	No
Workstation	1	1	230 V	No
Additional parts	1	1	230 V	No
Total	19	14 kW, 16×[230 V] 85kW, 7×[400V / 32A]		
Total with contingency	– –	17 kW [230 V] 102kW [400V / 32A]		

Table 4: Electrical needs for the installation of the prototype at CERN

from the magnet. WS2 will contain the cryostat in parking position and all the electronic racks that would slide on dedicated rails. These rails will allow to avoid the necessity of unplugging all cables when the cryostat is sliding inside the magnet bore. In contrary, the interferometer and motor racks will be unplugged and moved downstream when the cryostat will be inside the magnet. This requires a platform downstream at the same height as upstream with an area of 3×3 m^2. The compressors needed for the cryogenics do not have to be on the upstream platform – instead they will be put on the floor, behind the magnet.

This floor map is presently being discussed with the H8 CERN North Area responsible and may be subject to (slight) changes.

5.6 Planning of operation

The phase of installation consists of cleaning the area, installation of sliding rails [6], building of the tent, installation of the racks, installation of compressors and water chillers ... . To maximize time during the actual shutdown periods, these operations can take place in parasitic mode, so typically installation will start in e.g. October – to be adjusted depending on ATLAS needs. This phase of installation should end with a safety review.

[6] After dismounting of the current ATLAS rails.

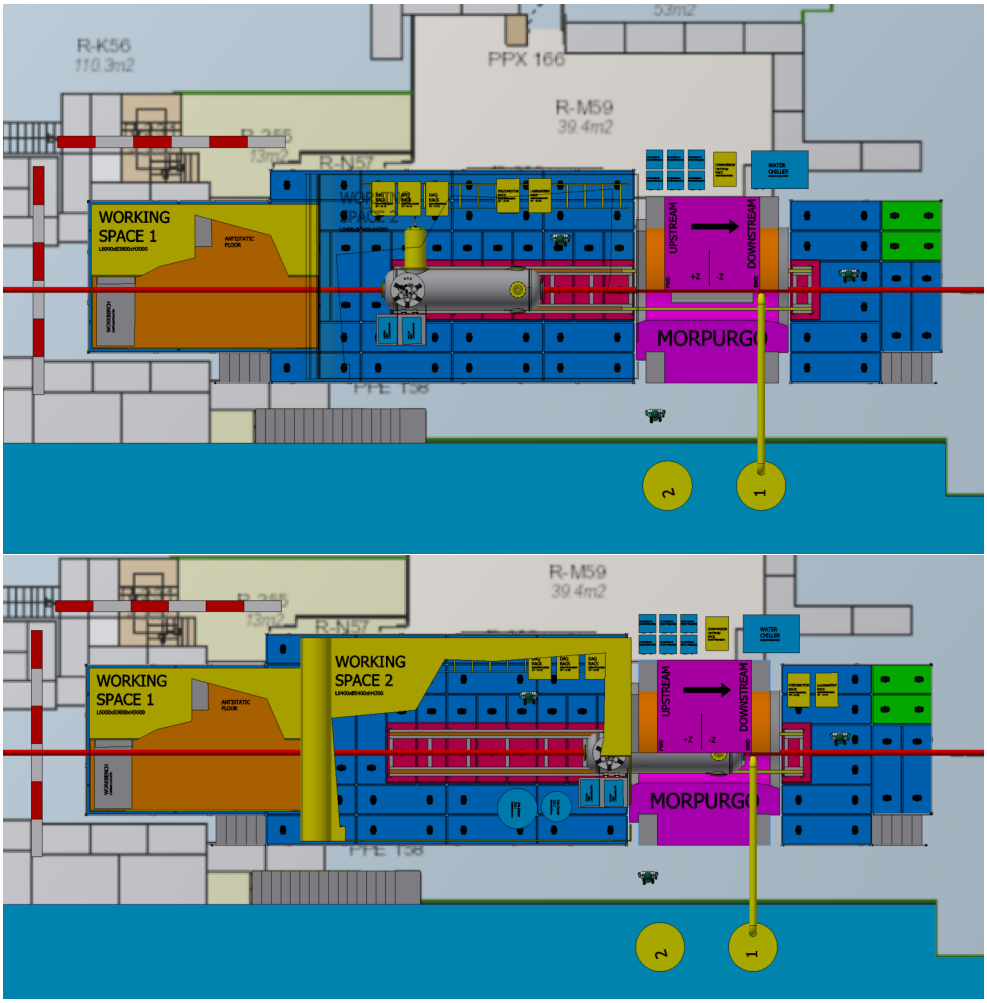

Figure 12: Proposed floor plan around MORPURGO to allow for the installation of MADMAX prototype. For clarity the working space 2 is not shown. Top) parking position. Bottom) Inside the magnet.

Early December, the cryostat and the booster will be shipped from Hamburg to CERN. The cryostat will be put on the sliding rails with the crane. The tent will be closed to allow for booster assembly and installation in the cryostat.

In January, the cryostat will be slided inside MORPURGO and cooled down, while the magnet is prepared (this takes 3 weeks). February and March are devoted to mechanical tests and, once these are completed, to physics runs with the magnet on. In April, the cryostat will be warmed up, slided out of MORPURGO and put in parking position. The booster is extracted. Finally, the tent and the rails will be dismounted, stored in the North Area and the original rails can be put back. The cryostat will be shipped back to Hamburg with all electronic racks. These operations should take around two weeks in total.

Recent discussion with CERN representatives confirmed that the (room temperature) gas supply, general electricity supply, de-mineralized cooling water circuit and magnet

operation system will be available during the shutdowns. The cryogenic services will also be available during the shutdowns between January and April, which matches our schedule. Similarly, the MORPURGO magnet will be available from January onwards [7]

5.7 Milestones and tentative time schedule

The time schedule of the MADMAX prototype experiment is driven by the R&D needed for some booster components (especially piezo motors and disk tiling development) and procurement of the cryostat. A tentative time schedule denoting the most important milestones is shown in Fig. 13. First usage of the MORPURGO magnet is planned during the 2021-2022 shut down, when already available sub-components of the booster may be tested without the cryostat.

Note that there is the risk that components to be developed will need more R&D iterations than initially thought. This implies that the schedule at present stage can't be guaranteed. It will be regularly updated on a half-yearly basis. It is well possible that measurements may continue after 2024.

6 Summary and conclusions

The MADMAX collaboration is devoted to the challenging task of detecting the dark matter axion in the mass range around 100 μeV. The experiment will be based on the concept of the dielectric haloscope.

Investigations show that MADMAX could indeed reach the sensitivity needed to discover axion dark matter. While challenging, the production of the setup with the needed accuracy seems feasible.

The development of the different components of the setup are ongoing. As a first step towards realization, a down-scaled prototype experiment will be built. It is expected that this setup will be available in 2022. It will be used for extensive testing and understanding of the mechanical principles, as well as the RF behavior of such a system. Extensive tests inside the MORPURGO magnet at CERN are planned. These are essential for verification of the feasibilty of the concept and are expected to give important inputs towards the design of the final experimental setup. Also it is planned to use the measurements with the MADMAX prototype inside the MORPURGO magnet for first physics measurement. These would provide competitive limits for ALPs in a yet unexplored mass range.

We ask the CERN SPSC to endorse the plans of the MADMAX collaboration to use the MORPURGO dipole magnet at North Area of CERN to perform first ALP search in a so far unexplored parameter range, after having validated the feasibility of operating the prototype in a strong B-field.

[7] Due to consolidation, MORPURGO will only be available during the last couple of weeks of the 2021-2022 shutdown.

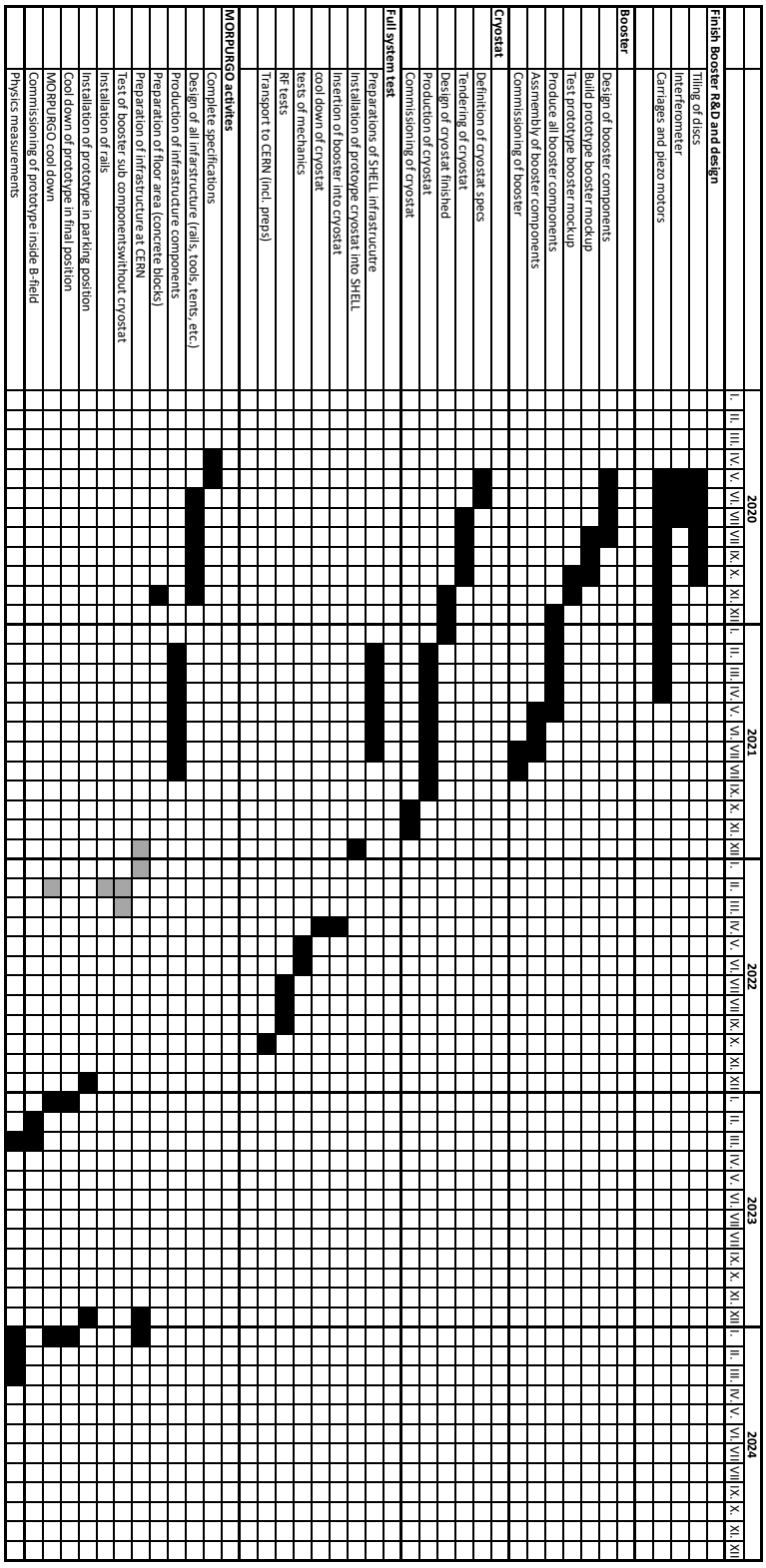

Figure 13: Time schedule for the MADMAX prototype and its implementation at CERN to the MORPURGO surrounding.

References

[1] A. Caldwell *et al.*, Phys. Rev. Lett. **118** (2017) 091801, [arXiv:1611.05865]

[2] A.J. Millar *et al.*, J. Cosmol. Astropart. Phys. **01** (2017) 061, [arXiv:1612.07057]

[3] A.N. Ioannisian *et al.*, J. Cosmol. Astropart. Phys. **09** (2017) 005, [arXiv:1707.00701]

[4] A.J. Millar, J. Redondo and F.D. Steffen, J. Cosmol. Astropart. Phys. **10** (2017) 006, Erratum ibid. **1805** (2018) E02, [arXiv:1707.04266]

[5] J. Egge, S. Knirck, B. Majorovits, C. Moore and O. Reimann, [arXiv:2001.04363]

[6] PRC review committee,

https://prc.desy.de/sites2009/site_prc/content/e38/e174111/e283187/infoboxContent294114/MADMAX_review_recommendations_12112019_final.pdf

[7] C.A. Baker *et al.*, Phys. Rev. Lett. **97** (2006) 131801, [arXiv:hep-ex/0602020]

[8] J. M. Pendlebury *et al.*, Phys. Rev. D **92** (2015) 092003 [arXiv:1509.04411].

[9] R.D. Peccei and H.R. Quinn, Phys. Rev. Lett. **38** (1977) 1440

[10] R.D. Peccei and H.R. Quinn, Phys. Rev. D **16** (1977) 1791

[11] S. Weinberg, Phys. Rev. Lett. **40** (1978) 223

[12] F. Wilczek, Phys. Rev. Lett. **40** (1978) 279

[13] G. Grilli di Cortona *et al.*, J. High Energy Phys. **1601** (2016) 034, [arXiv:1511.02867]

[14] G. Raffelt, Lect. Notes Phys. **741** (2008) 51, [arXiv:hep-ph/0611350]

[15] J.H. Chang, R. Essig and S.D. McDermott, J. High Energy Phys. **1809** (2018) 051, [arXiv:1803.00993]

[16] M. Giannotti *et al.*, J. Cosmol. Astropart. Phys. **1710** (2017) 010, [arXiv:1708.02111]

[17] J. Preskill, M.B. Wise and F. Wilczek, Phys. Lett. B **120** (1983) 127

[18] L.F. Abbott and P. Sikivie, Phys. Lett. B **120** (1983) 133

[19] M. Dine and W. Fischler, Phys. Lett. B **120** (1983) 137

[20] M. Kawasaki, K. Saikawa and T. Sekiguchi, Phys. Rev. D **91** (2015) 065014, [arXiv:1412.0789]

[21] T. Hiramatsu *et al.*, Phys. Rev. D **85** (2012) 105020, Erratum ibid. **86** (2012) 089902, [arXiv:1202.5851]

[22] A. Ringwald and K. Saikawa, Phys. Rev. D **93** (2016) 085031, Erratum ibid. **94** (2016) 049908, [arXiv:1512.06436]

[23] L. Fleury and G.D. Moore, J. Cosmol. Astropart. Phys. **1601** (2016) 004, [arXiv:1509.00026]

[24] L.M. Fleury and G.D. Moore, J. Cosmol. Astropart. Phys. **1605** (2016) 005, [arXiv:1602.04818]

[25] G.D. Moore, [arXiv:1604.02356]

[26] V.B. Klaer and G.D. Moore, J. Cosmol. Astropart. Phys. **1711** (2017) 049, [arXiv:1708.07521]

[27] M. Gorghetto, E. Hardy and G. Villadoro, J. High Energy Phys. **1807** (2018) 151, [arXiv:1806.04677]

[28] S. Borsanyi *et al.*, Nature **539** (2016) 69, [arXiv:1606.07494]

[29] D. Horns *et al.*, J. Cosmol. Astropart. Phys. **1304** (2013) 016, [arXiv:1212.2970]

[30] J. Jaeckel and J. Redondo, Phys. Rev. D **88** (2013) 115002, [arXiv:1308.1103]

[31] O.C. Zienkiewicz, "The finite element method", McGraw-Hill London, 1977

[32] COMSOL Multiphysics® v. 5.3.a, COMSOL AB, Stockholm, Sweden, www.comsol.com

[33] Elmer – Finite Element Solver for Multiphysical Problems, www.csc.fi/web/elmer/elmer

[34] J. E. Kim, Phys. Rev. Lett. **43** (1979) 103; M. A. Shifman, A. I. Vainshtein and V. I. Zakharov, Nucl. Phys. B **166** (1980) 493

[35] A.P. Zhitnitskii, Sov. J. Nucl. Phys. **31** (1980) 260; M. Dine, W. Fischler and M. Srednicki, Phys. Lett. B **104** (1981) 199

[36] V. Anastassopoulos *et al.*, Nature Phys. **13** (2017) 584, [arXiv:1705.02290]

[37] W. Chung, DESY-PROC-2017-02

[38] IAXO collaboration, J. Cosmol. Astropart. Phys. **1906** (2019) 047, [arXiv:1904.09155]

[39] See ALPS-II webpage, https://alps.desy.de/e191931/

[40] See BRASS webpage, http://www.iexp.uni-hamburg.de/groups/astroparticle/brass/brassweb.htm

[41] L. Di Luzio, F. Mescia and E. Nardi, Phys. Rev. Lett. **118** (2017) 031801, [arXiv:1610.07593] and L. Di Luzio, F. Mescia and E. Nardi, Phys. Rev. D **96** (2017) 075003, [arXiv:1705.05370]

[42] C. Hagmann *et al.*, Phys. Rev. D **42** (1990) 1297

[43] W. Wuensch *et al.*, Phys. Rev. D **40** (1989) 3153

[44] MADMAX collaboration, Eur. Phys. J. C **79** (2019) 186, [arXiv:1901.07401]

[45] F. Beaujean, A. Caldwell and O. Reimann, Eur. Phys. J. C **78** (2018) 793, [arXiv:1710.06642]

[46] S. Knirk, PhD Thesis, Technicshe Uinversität München, 2020.

[47] M. Teuwen *et al.*, Proc. SPIE **6269** (2006) 62694B-1

[48] A. Mato Martínez *et al.*, Proc. SPIE **9912** (2016) 99121A-1

[49] M. Morpurgo, Cryogenics **19** (1979) 411

[50] M. Rosenthal *et al.*, CERN-ACC-NOTE-2018-0028, http://cds.cern.ch/record/2310483

[51] B. Majorovits, P. Pralavorio and J. Schaffran, CERN-SPSC-2019-021, http://cds.cern.ch/record/2676670

[52] A. Dudarev, private communication